雑誌

Suzuki K., Kawamura Y., Hayashi T., SakuraiT., Hasegawa Y., Sankai Y.	Intention-Based Walking Support for Paraplegia Patient	Proc. of Int'l Conf. on Systems, Man and Cybernetics (SMC2005)		2707-2713	2005
葛岡英明, 山崎敬一, 上坂純一	ロボットを介した遠隔コミュニケーションシステムにおけるエコロジーの二重性の解決：頭部連動と遠隔ポインタの評価	情報処理学会論文誌	46(1)	187-196	2005
山越恭子, 葛岡英明	言葉を使用したワークリズム提示手法の提案	ヒューマンインタフェース学会・論文誌	7(1)	121-130	2005
酒田信親, 蔵田武志, 興梠正克, 葛岡英明, マーク・ビリングハースト	肩載せアクティブカメラ・レーザによる遠隔協調作業	日本VR学会論文誌	10(3)		2005
檜山敦, 山下淳, 西岡貞一, 葛岡英明, 広田光一, 広瀬通孝	「ユビキタスゲーミング」位置駆動型モバイルシステムを利用したミュージアムガイドコンテンツ	日本VR学会論文誌	10(4)	523-532	2005
Hideaki Kuzuoka, Jun Yamashita, Keiichi Yamazaki, Tetsuo Yukioka, Shoichi Ohta, Paul Luff	Working Hands: Embodying Interaction for Healthcare	ECSCW 2005		125-127	2005
中島孝	神経難病における遺伝子検査とインフォームドコンセント	神経治療学			2005
中島孝	難病ケアと問題点－QOLの向上とは	臨床神経学			2005
中島孝	ALSのQOL向上と緩和ケア	医療			2005
Atsushi Miki, Takashi Nakajima, Mineo Takagi, Tomoaki Usui, Haruki Abe, Chia-Shang J. Liu, BA, and Grant T. Liu, MD	Near-infrared Spectroscopy of the Visual Cortex in Unilateral Optic neuritis	Am J Ophthalmol	139	353-356	2005
中島孝	難病の生活の質（QOL）研究で学んだこと　―　課題と今後の展望	JALSA	64	51－57	2005

雑誌

中島孝	生をささえる共通基盤をもとめて－QOLの価値観は健康時から重症時へとどんどん変化していく	難病と在宅ケア	10(12)	7-12	2005
梶間日出輝, 長谷川泰久, 福田敏男	マルチロコモーションロボットによるブラキエーション運動制御 -エネルギーに基づくSwing-back制御-	日本ロボット学会誌	23(8)	993-1001	2005

IV. 研究成果の刊行物・別刷り

Advanced Robotics, Vol. 19, No. 9, pp. 977–993 (2005)

Also available online - www.vsppub.com

Full paper

Three-dimensional link dynamics simulator based on *N*-single-particle movement

HIDEKI TODA * and YOSHIYUKI SANKAI

Doctoral Program of Systems and Information Engineering, Sankai Laboratory, University of Tsukuba, Tsukuba, Ibaraki, 305-0006, Japan

Received 31 August 2004; accepted 14 October 2004

Abstract—The purpose of this paper is to suggest a new three-dimensional multi-link system dynamics simulator. A 'Jacobian' matrix was generally used for calculating the dynamics of the multi-link system in previously proposed methods; however, this method has many difficulties related to the computational cost and precision of the calculations. For example, there are the problems of the singularity and the accumulation of calculation errors when it follows from the root to the end of the link, and the problems of treating external force effects in the angular space dynamics. In this study, we consider a multi-link system as a multi-particle movement system and each of the particles are connected by a kind of spring damper model as an imitation of a link. Using this mechanism, the Jacobian matrix is not required in the dynamics simulation and the complexity of the link dynamics simulation is dramatically decreased by way of introducing a rotational plane concept. We confirm the effectiveness of the simulator through some dynamics simulations such as walking.

Keywords: Three-dimensional multi-link simulator; robot control; link dynamics.

1. INTRODUCTION

Many multi-joint type robot systems have been recently proposed (WABIAN [1], HRP [2], ASHIMO [3], KHR-1 [4]) and used with the aim of imitating human movement [5]. The rationale for imitating human movement is to acquire a new movement which was impossible in previous studies and to search for a generating or learning mechanism of the movement which is closer to that of a human being. For realizing human movement, however, it is necessary to introduce expensive real robot systems and to prepare the environment of the system at the same time. In addition, we must include an algorithm to realize a task into the control system and confirm the effectiveness step by step. In this case, physical problems with the control system and performance deterioration of the motors or actuators can

*To whom correspondence should be addressed. E-mail: toda@golem.kz.tsukuba.ac.jp

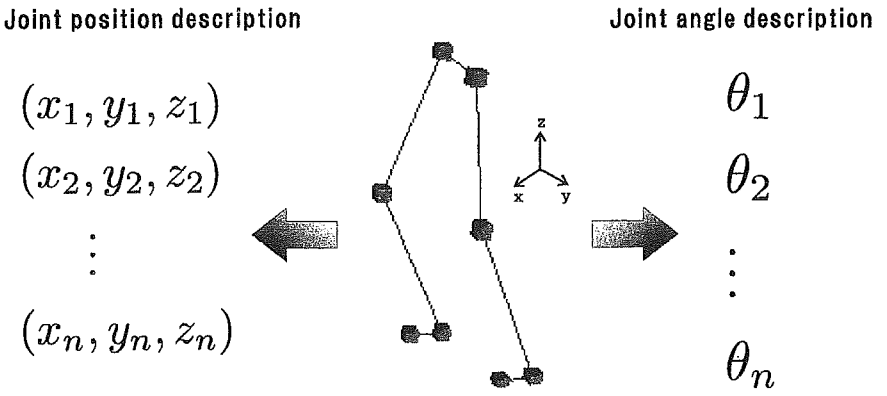

Figure 1. Joint position and angle description.

cause serious difficulties. When the movement does not go well, it is difficult to analyze it and understand if the reason lies in the control algorithm or the physical structure (kinematics) of the robot. If the purpose of using a real-world robot depends on ascertaining the role of the control algorithm and the effect through the experiments, the practical working difficulties will be equivalent to the cost of manufacturing an atomic bomb and ascertaining the explosive power. In addition, destructive influences such as a turnover or shock become very important factors and environmental effects such as the influence of the ground conditions (sandy or muddy) also become important when we consider the safety of the robot system.

Generally, in order to reduce experimental cost, a virtual world computer simulation (e.g. Open-HRP [6, 7], Human Figure [8]) or another mathematical calculation method [9, 10] is used. However, it produces some difficulties because precise modeling of the external environment and robot system itself is difficult. The major reasons depend on the fundamental principle of conversion equivalence between the work space coordination $\vec{x}$ and the angle state space $\vec{q}$, and this principle assures that we can change the work space coordinate into the angle state space coordinate, which is convenient for the calculation. However, this conversion has a singularity — in the case that there is no inverse matrix. In addition, there are problems of introducing external effects into the angular space dynamics and an accumulation of calculation errors when it follows from the root to the end of the link. In particular, influences of external forces or effects to be added in the link system often appear in the form of 'condition of the ground', 'shock from the external environment' or 'link vibration and distortion', and these influences are directly connected to the stability of the system. Each time these external factors increase, the influences must be analyzed and added into the link dynamics simulator in order to understand the dynamics phenomenon in the angular state space. For example, in the case of introducing unstable soft ground into the simulator, we must know the influence of the collision effect when a link touches ground and the effect of the ground motion itself. These factors are analyzed and added mathematically in the angular state space. In short, the dynamics phenomenon on the work space coordinate is difficult to convert into the angle state space. In almost all of the cases, these analysis and

conversion processes are very complex, and the precision of the simulation of the dynamics has fallen through the process of simplification. Each time we want to add environmental factors into the simulator, we must repeat these processes and reduce the degree of freedom of the simulator against the environments. These processes cause a heavy calculation load and the precision of the calculation is thus reduced. In this study, we propose a new multi-link dynamics simulator system which does not need to use the 'Jacobian' conversion process from work space to angle space or from angle space to work space in the link dynamics calculation. Our proposed method considers that the multi-link system is equivalent to a multi-particle system in which each of the particles is restricted by other particles. In other words, the system in which each of the particles is connected with a spring–damper model is considered as an approximation of the link movement in our method. Using this approximation, the amount of calculation is reduced dramatically and it is easy to introduce external dynamic factors of the environment in the proposed method.

2. DYNAMIC LINK MODEL DESCRIPTION

The proposed multi-link system description method does not utilize the angular expression method of the rigid body system which is used to describe the link dynamics in the previously proposed method. It does not use the joint angle state space, except when necessary. The position relation of the joint on the work space is used in order to describe the joint angle. An expression of the joint angle becomes possible if there are at least three points on the work space as shown in Fig. 2a. We consider that each of the points is connected by some kind of restriction condition. Although any kind of restriction condition may be used, we selected the spring–damper model as the restriction condition due to reasons of simplicity and stability (Fig. 2b).

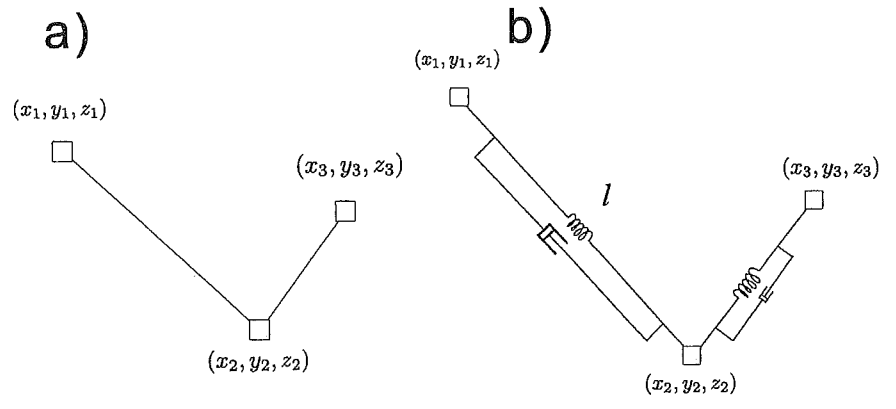

Figure 2. Link position description as a spring–damper model.

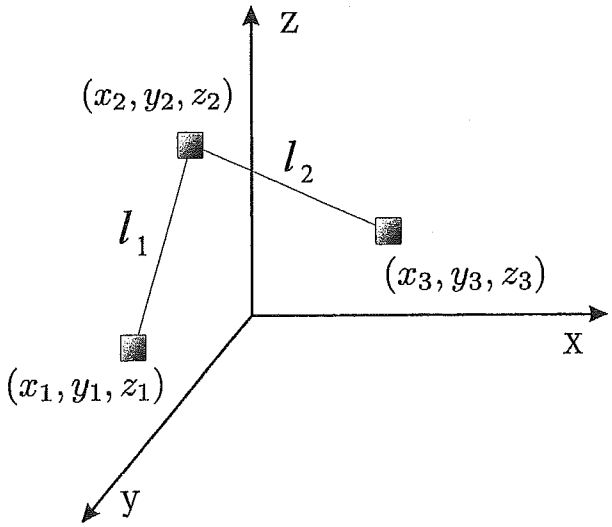

Figure 3. The joint representation constructed from three particle points.

Each particle receives some force from the other particles under the conditions of presuming a spring–damper model and this system cannot move in any free direction.

As shown in Fig. 3, one joint is constructed when one particle is restricted at a distance l from the other two particles. This restriction condition is very important for treating rigid body dynamics as 'the system has the size'. For introducing the motion equation of the multi-link system under the restriction condition of the spring–damper, we define the Lagrangian of the system with only three particle points in the three-dimensional space:

$$\begin{aligned} L &= T - G \\ &= \frac{1}{2}m_1\dot{\vec{x}}_1^2 + \frac{1}{2}m_2\dot{\vec{x}}_2^2 + \frac{1}{2}m_3\dot{\vec{x}}_3^2 - \frac{1}{2}K\Delta l_1^2 - \frac{1}{2}K\Delta l_2^2 \end{aligned} \tag{1}$$

where $\vec{x}_1 = (x_1, y_1, z_1)$, $\vec{x}_2 = (x_2, y_2, z_2)$, $\vec{x}_3 = (x_3, y_3, z_3)$, L is the Lagrangian, T is the kinetic energy, G is the potential energy of the spring, K is the friction coefficient of the damper 1 and damper 2, and m_1, m_2 and m_3 are equal to mass of each particle. We define Δl_1 and Δl_2 as:

$$\begin{aligned} \Delta l_1 &= l_1 - |\vec{x}_1 - \vec{x}_2| \\ \Delta l_2 &= l_2 - |\vec{x}_3 - \vec{x}_2| \end{aligned} \tag{2}$$

Using the method of the Euler–Lagrange equation:

$$\frac{\partial L}{\partial \dot{\vec{x}}_1} = m_1\dot{\vec{x}}_1 \tag{3}$$

$$\frac{\partial L}{\partial \vec{x}_1} = 2K(\vec{x}_1 - \vec{x}_2) \cdot \left[1 - \frac{l_1}{|\vec{x}_1 - \vec{x}_2|}\right] \tag{4}$$

The motion equation $\vec{x}_1$ of the particle 1 is:

$$\frac{d}{dt}\frac{\partial L}{\partial \dot{\vec{x}}_1} - \frac{\partial L}{\partial \vec{x}_1} = 0 \tag{5}$$

That is:

$$m_1 \ddot{\vec{x}}_1 = -2K(\vec{x}_1 - \vec{x}_2) \cdot \left[1 - \frac{l_1}{|\vec{x}_1 - \vec{x}_2|}\right] \tag{6}$$

By defining $l_{12} = |\vec{x}_1 - \vec{x}_2|$, we obtain:

$$m_1 \ddot{\vec{x}}_1 = -2K(\vec{x}_1 - \vec{x}_2)\left[1 - \frac{l_1}{l_{12}}\right] \tag{7}$$

The singular point is created when the position $\vec{x}_1$ equals $\vec{x}_2$. However, because the two particle positions are thought to be connected with a spring, we can consider that the singular point is not created. It only occurs under a large external force, with the spring completely contracted.

Other coordinate motion equations are represented as:

$$m_1 \ddot{\vec{x}}_1 = -2K(\vec{x}_1 - \vec{x}_2)\left[1 - \frac{l_1}{l_{12}}\right] \tag{8}$$

More importantly, the effect of the number of restriction conditions directly appears in the Lagrangian function as simply increasing the number of terms and it appears in the motion equation as simply increasing the number of terms. For example, the motion equation of particle 2 is represented as:

$$\begin{aligned} m_2 \ddot{\vec{x}}_2 = &+2K(\vec{x}_1 - \vec{x}_2)\left[1 - \frac{l_1}{l_{12}}\right] \\ &-2K(\vec{x}_3 - \vec{x}_2)\left[1 - \frac{l_2}{l_{23}}\right] \end{aligned} \tag{9}$$

where l_{23} is the distance between particles 2 and 3. The motion equation of particle 3 is:

$$m_3 \ddot{\vec{x}}_3 = -2K(\vec{x}_3 - \vec{x}_2)\left[1 - \frac{l_2}{l_{23}}\right] \tag{10}$$

We can understand that (9) has two spring–damper restriction conditions from particles 1 and 3, and (10) has one restriction condition from particle 2. This means that the number of restriction conditions never increases the complexity of the motion equation and is directly proportional to the number of restriction conditions.

When we consider the motion dynamics by using the angular state space, we need to resolve the angular acceleration level dynamics of the system. If the dynamics include the free work space movement, the description will be complicated by the center of mass movement and the rotation or relative movement. However, our proposed method does not need to consider those coordinate conversions. For

example, a fixed position can be described very simply by way of $\dot{\vec{x}}_i = 0$ and $\ddot{\vec{x}}_i = 0$, but these restriction conditions are difficult to treat in the angular state space description. In addition, our approach does not depend on whether a link is closed or open at all, e.g., the open link in Fig. 3 can converted into a closed link by connecting the joint coordinates 1 and 3 by a spring–damper; motion equations (8) and (10) just have two terms, respectively, such as in (9) and the unstable computational structure does not occur:

Our proposed method is very simple, but there are some difficulties:

(i) Each particle position has a small vibration.

(ii) There is no rotation restriction of the joint.

(iii) It cannot represent the torque or the friction effects in the system.

Below, we describe each of these points.

3. THE DEFINITION OF THE ROTATION PLANE

Since each particle is connected by the spring system, the first problem is clear. However the vibration effects can be inhibited by using other factors such as compliance or friction effects of the spring system. If vibration does occur, the conservation of mechanical energy of the link system is not maintained. In real world motion dynamics, energy dissipation occurs in the aluminum or iron link, and we can explain that the dissipation is converted to internal grid motion and disappears as thermal energy. In addition, we can introduce a very large external impulse by using the solid-state properties such as 'thermal' effects or expansion or contraction.

The next problem is rotation restriction. The joint movement equations (8)–(10) represent 'spherical joint' dynamics, such as in a hip joint, but a general serial link has only one motor and is restricted to a single rotation axis. Figure 4 represents three particles and a surface which is spanned by the three points. We define this surface as the 'rotation plane'. The surface has a normal vector $\vec{n}$ and we construct the restriction that the three particles can move only in the rotation plane.

First, we calculate $\ddot{\vec{x}}_1$, $\ddot{\vec{x}}_2$ and $\ddot{\vec{x}}_3$ of the three particles. Next, we delete the acceleration factor parallel to the normal vector (Fig. 5). For example, by using the normal vector $\vec{n}$ and $|\vec{n}| = 1$, the acceleration factor parallel to $\vec{n}$ is represented as:

$$\vec{a}^n = (\vec{n} \cdot \vec{a}_1)\vec{n} \tag{11}$$

By deleting the parallel factor:

$$\vec{a}^{\text{new}} = \vec{a} - \vec{a}^n = \vec{a} - (\vec{n} \cdot \vec{a})\vec{n} \tag{12}$$

The acceleration term $\vec{a}^{\text{new}}$ is used instead of $\vec{a}$. We can define the rotation joint which has a single rotation axis by using this process.

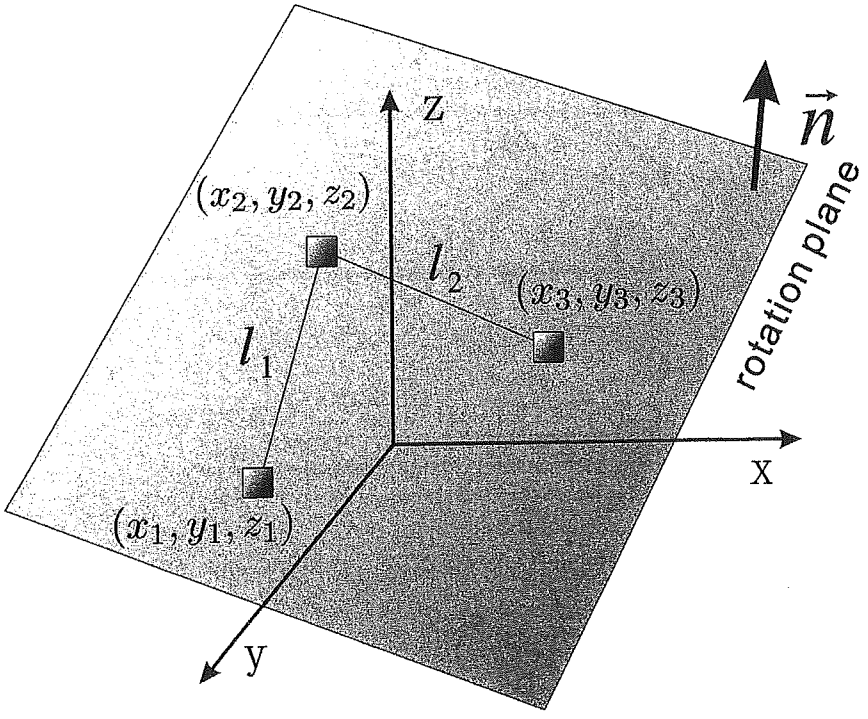

Figure 4. Rotation plane.

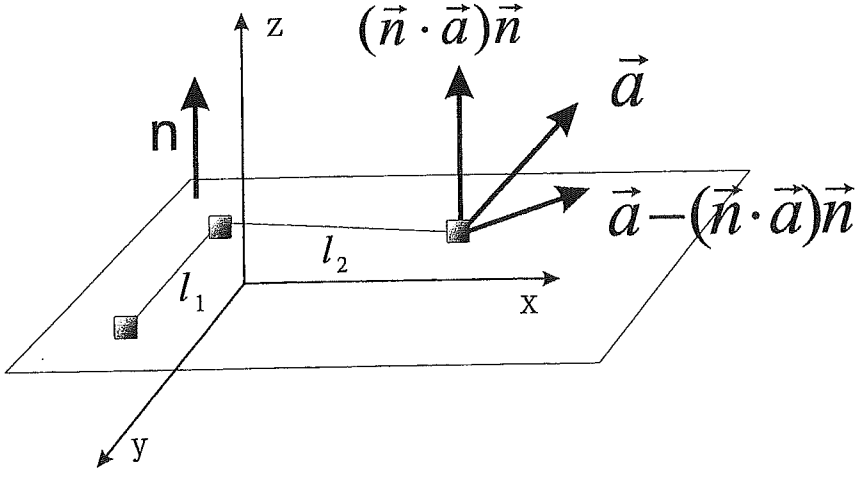

Figure 5. Acceleration decomposition.

3.1. Torque effect

For simplifying the torque effect descriptions of the joint movement, we consider the one-dimensional space movement of two particles (Fig. 6). There is no friction in the system, and the two particles are in touch with the spring and not connected to each other. If the spring becomes stretched, the two particles move separately. This shows that there is no center of mass movement and that only relative movement has occurred (Fig. 6c).

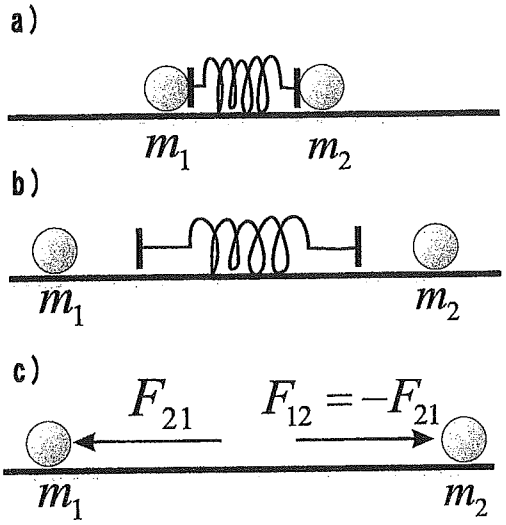

Figure 6. One-dimensional movement of two particles. (a) Initial state. (b) The presence of internal force. (c) $F_{12} = -F_{21}$.

The motion equation is:

$$m_1\ddot{x}_1 = F_{21} + F_1^{ex} \tag{13}$$

$$m_2\ddot{x}_2 = F_{12} + F_2^{ex} \tag{14}$$

where F_1^{ex} is the external force to particle 1 and F_{21} is the internal force, and there is a simple relationship $F_{21} = -F_{12}$. That is the law of action and reaction. We consider the case of $F_1^{ex} = 0$ and $F_2^{ex} = 0$, and the relative movement equation $x = x_1 - x_2$ is:

$$\frac{m_1 m_2}{m_1 + m_2}\ddot{x} = F_{12} \tag{15}$$

where μ means the conversion mass $\mu = \frac{m_1 m_2}{m_1 + m_2}$:

$$\mu\ddot{x} = F_{12} \tag{16}$$

When we apply it to the rotation movement, the key point is that the internal force F_{12} is equivalent to the torque effect and it is the force which tries to open a joint angle as an internal force. We can consider this situation in the rotation movement, where the motion equation is:

$$I_1\ddot{\theta}_1 = \tau_{21} = \tau \tag{17}$$

$$I_2\ddot{\theta}_2 = \tau_{12} = -\tau \tag{18}$$

where I_1 and I_2 are of the momentum values and θ_1 and θ_2 are the rotation angles of mass 1 and 2. The important point is that the torque τ can be treated as an internal force and we can separate it in to the movement of two particles (Fig. 7).

The force f_1 which is generated by the torque τ in a distance l_1 (Fig. 8):

$$f_1 = \frac{\tau}{l_1} \tag{19}$$

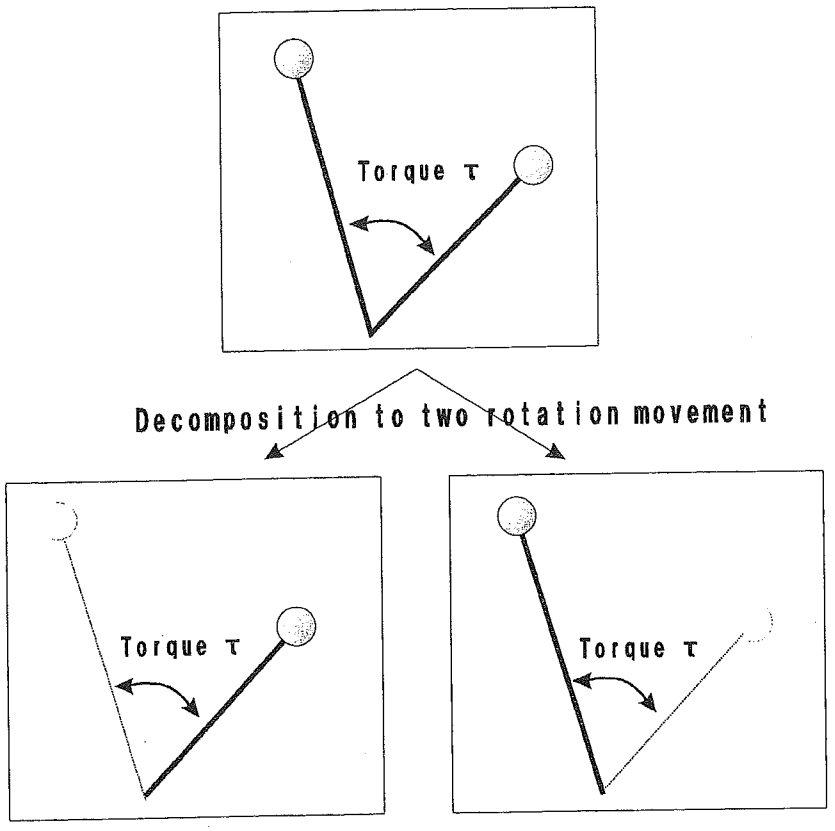

Figure 7. Relative rotational movement and internal force (torque).

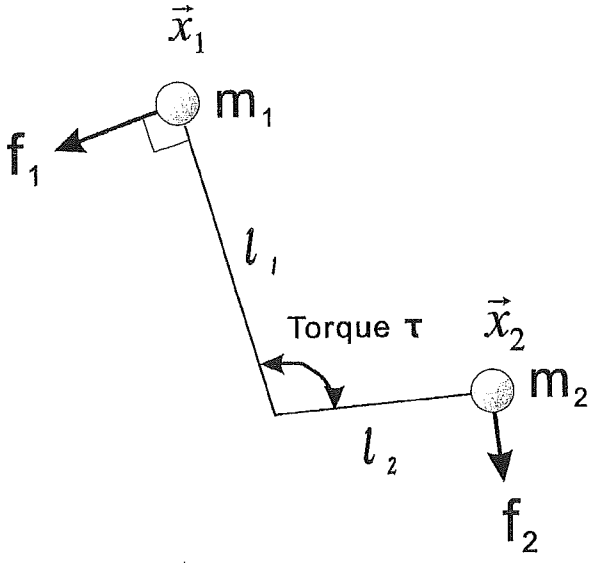

Figure 8. Influence on the two particles by the torque effect.

In general:

$$\vec{f}_1 = \frac{\tau}{l_1^2}\vec{n} \times \vec{x}_1 \tag{20}$$

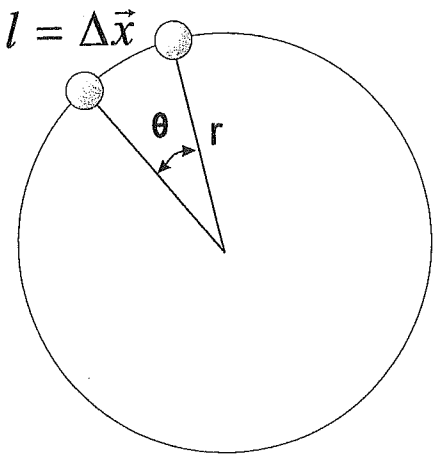

Figure 9. Rotation angle and angular velocity.

where $\vec{n}$ is the normal vector of the rotation plane, $\vec{x}_1$ is the position of the particle from the rotation center and l is the distance $l = |\vec{x}_1|$.

Two particles are effected by $\vec{f}_1$ and $\vec{f}_2$ calculated from Fig. 8:

$$\vec{f}_1 = \frac{\tau}{l_1^2}\vec{n} \times \vec{x}_1, \quad \vec{f}_2 = \frac{\tau}{l_2^2}\vec{n} \times \vec{x}_2 \tag{21}$$

By using this decomposition process, we can convert the torque effect to the force toward the two particles and we can describe the torque effect of the joint.

3.2. *Friction effect*

The next process is to describe the friction effect of the joint in the rotation movement. First, the friction effect is represented as:

$$\tau = -D\dot{\theta} \tag{22}$$

where D is the friction coefficient, θ is the rotation angle and τ is the torque. It is clear that $l = r \cdot \theta$ (Fig. 9):

$$\Delta l = r \cdot \dot{\theta} = \Delta\vec{x} \sim \dot{\vec{x}} \tag{23}$$

in the case of a very small time step.

In addition, by including the fact that one joint is constructed from three particle coordinates, the particle position $\vec{x}_1$, $\vec{x}_2$'s angular velocity $\vec{\theta}_1$, $\vec{\theta}_2$ seen from the rotation center $\vec{x}_2$ is directly connected with the joint angle velocity $\vec{\theta}$:

$$\dot{\theta}_1 = \frac{\Delta\vec{x}_1}{l_1} \sim \frac{\dot{\vec{x}}_1}{l_1}, \quad \dot{\theta}_2 = \frac{\Delta\vec{x}_2}{l_2} \sim \frac{\dot{\vec{x}}_2}{l_2} \tag{24}$$

The torque value calculated from the friction effect of the joint is:

$$\tau^{\text{friction}} = -\frac{D}{l_1}(\dot{\vec{x}}_1 - \dot{\vec{x}}_2) \tag{25}$$

$$-\frac{D}{l_2}(\dot{\vec{x}}_3 - \dot{\vec{x}}_2) \tag{26}$$

By adding this effect to (21), we can include the friction effect in the multi-link movement dynamics.

4. SINGLE-LINK MOVEMENT CONTACT WITH FLOOR

In this section, we simulate a single-link system movement which is constructed from three particles, and confirm it under the condition of a free-fall state to touch and bounce off the floor. Figure 10 shows the movement of the single-link system. In the first phase, the link system falls down due to gravity (phase 1). This effect is realized by adding the gravity effect to the motion equation:

$$m_i \frac{\mathrm{d}x^2}{\mathrm{d}t^2} = F_x \tag{27}$$

$$m_i \frac{\mathrm{d}y^2}{\mathrm{d}t^2} = F_y \tag{28}$$

$$m_i \frac{\mathrm{d}z^2}{\mathrm{d}t^2} = F_z + m_i g \tag{29}$$

where m_i is the mass of each of the particles, g is the gravity constant and (F_x, F_y, F_z) means the calculated force from (21) or spring–damper effect. The next phase is to touch the floor. The third particle contacts with and bounces off the floor. In this phase, we use the floor effect as:

$$\frac{\mathrm{d}z}{\mathrm{d}t} = \begin{cases} \dfrac{\mathrm{d}z}{\mathrm{d}t} & (z > \text{floor height}) \\ -0.8\dfrac{\mathrm{d}z}{\mathrm{d}t} & (z < \text{floor height}) \end{cases} \tag{30}$$

This is just an inelastic collision. In the third phase, the collision effect is transmited to other particles by the spring system and particle 2 shifts position to the right direction. In our proposed model, it is very easy to include these external effects as the force effect to each of the particles. For example, the effect of floor contact can be changed to an elastic collision, spring-type floor or non-linear deformation.

5. WALKING MOVEMENT OF THE HUMAN LINK MODEL

In this section, we construct an eight-particle link model which is shown in Fig. 11. This model has six rotation joints, p(1)–p(2)–p(3) represents a single joint, and each of the joints has friction and we can give a torque for each of the joints. The link length is 10 [p(1)–p(2) and p(8)–p(7):foot position], 50 [p(2)–p(3) and p(6)–p(7):leg], 40 [p(3)–p(4) and p(5)–p(6):hip], 20 [p(4)–p(5):hip joint width] in this

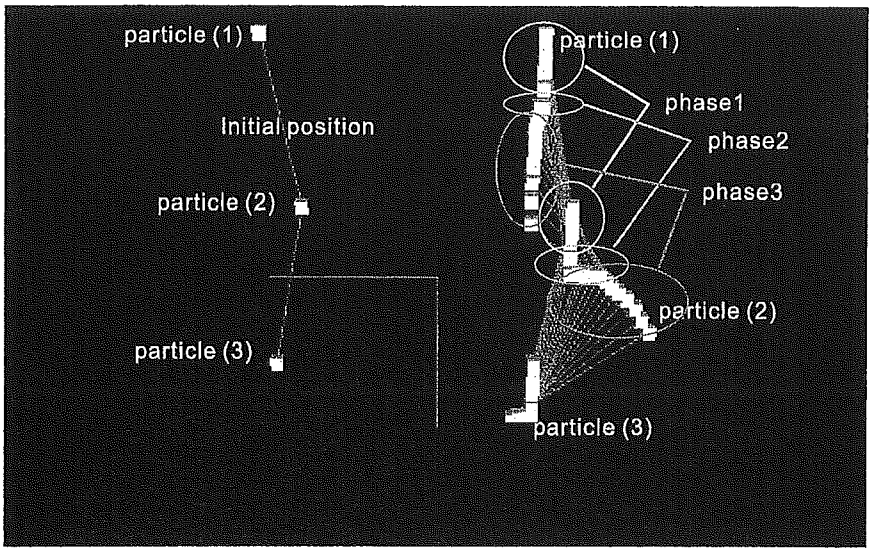

Figure 10. Single link movement contact with the floor under the effect of gravity.

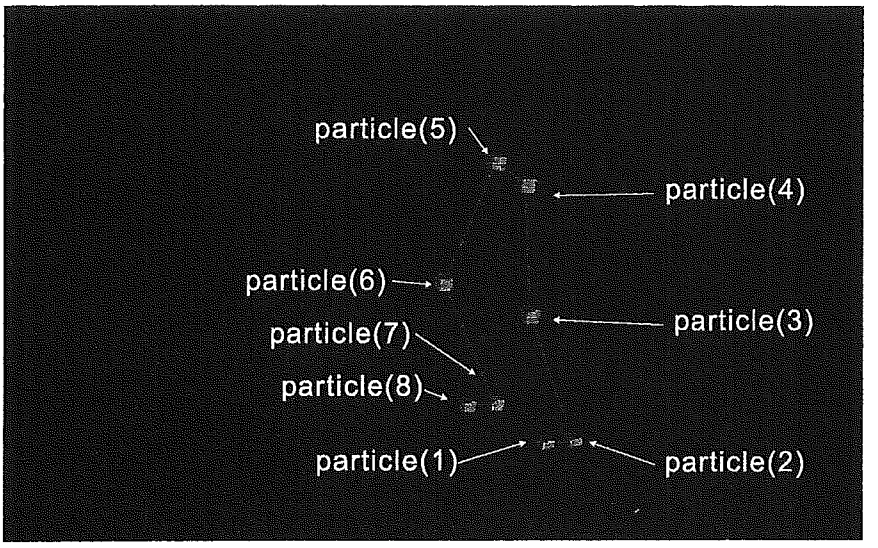

Figure 11. Human link model constructed of eight particles.

model (more detailed parameters are shown in Table 1). Figure 12 shows the free-fall phase of the simulation. The human model falls down and touches the floor. The floor is a simple spring system and each of the particles is effected by the criterion condition such as (30). We define the mass of the p(1)–p(3) and p(6)–p(8) as 1.0, and p(4)–p(5) as 10.0.

The next phase represents the walking movement in which the right leg is in the support phase and the left leg is in the swing phase (Fig. 13). In this simulation, the walking motion plan is given by an operator beforehand in order that the zero moment point [13] is under the foot's support polygon and each of the joint torques is determined by a simple PD feedback rule to realize the planned motion.

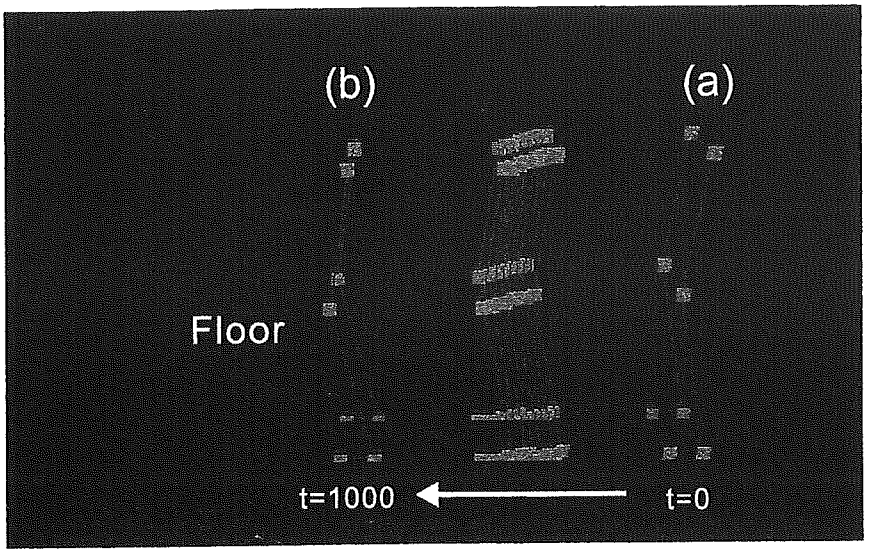

Figure 12. Free-fall phase. (a) Initial state ($t = 0$). (b) The model touches the floor and holds the standing state ($t = 1000$).

Table 1.
Precise model parameters

Parameter	Link connection	Value
Length	p(1)–p(2), p(7)–p(8)	10
Length	p(2)–p(3), p(6)–p(7)	50
Length	p(3)–p(4), p(5)–p(6)	40
Length	p(4)–p(5)	20
Mass	p(1)–p(3), p(6)–p(8)	1
Mass	p(4)–p(5)	10
Joint friction	p(1)–p(2)–p(3), p(2)–p(3)–p(4)	5.0
Joint friction	p(3)–p(4)–p(5), p(4)–p(5)–p(6)	5.0
Joint friction	p(5)–p(6)–p(7), p(6)–p(7)–p(8)	5.0

In order to realize forward walking movement of the human model, a friction effect formed by a foot contact with the floor is needed. If a particle is contacting with the floor (the walk direction is x) and the vertical component of the ground reaction force is T_z:

$$f_x = -\gamma \cdot \frac{\mathrm{d}x}{\mathrm{d}t} \cdot T_z \tag{31}$$

where f_x is the reaction force of the particle from the floor, γ is the friction drag and $\frac{\mathrm{d}x}{\mathrm{d}t}$ is the velocity. The ground reaction force is represented by:

$$T_z = \begin{cases} m_i \vec{a}_i \cdot \vec{n}_z & z \leqslant \text{floor height} \\ 0 & z > \text{floor height} \end{cases} \tag{32}$$

where $\vec{n}_z$ is the normal vector of the floor and $\vec{a}_i$ is the particle's acceleration.

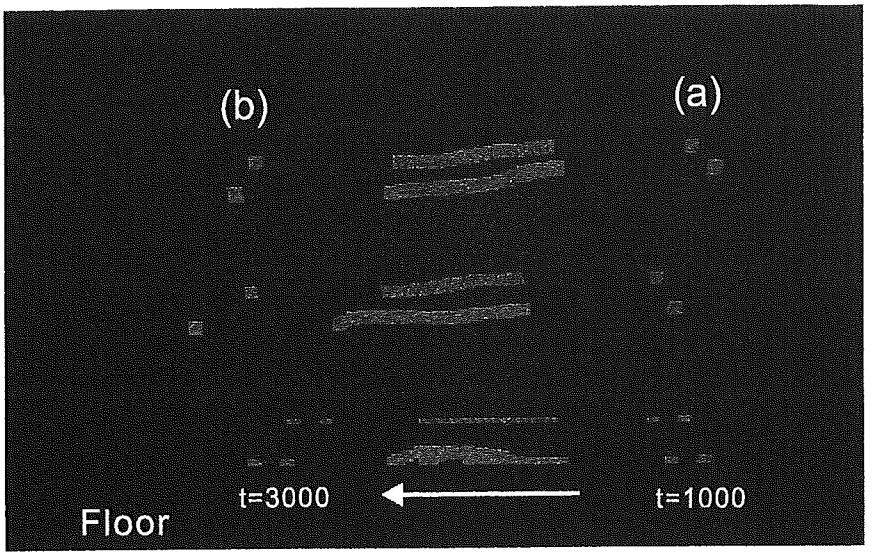

Figure 13. Walking movement phase 1. (a) Initial state ($t = 1000$). (b) Final state ($t = 3000$).

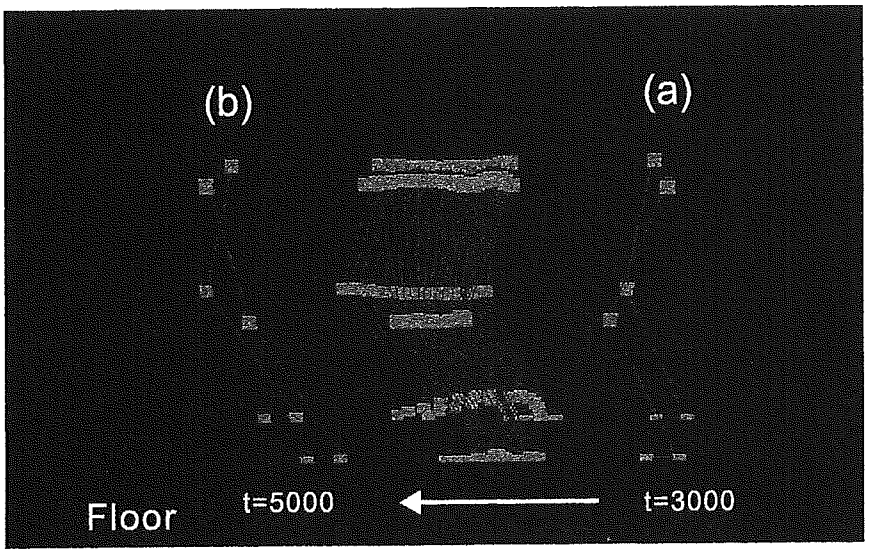

Figure 14. Walking movement phase 2. (a) Initial state ($t = 3000$). (b) Final state ($t = 5000$).

Figure 14 shows the walking movement when the right leg is in the swing phase and the left leg is in the support phase. The torque response curve of the support and the swing leg is shown in Fig. 15 from the free-fall phase ($t = 0 \rightarrow t = 1000$) to the first walking motion phase ($t = 1000 \rightarrow t = 3000$).

6. DISCUSSION

In our proposed model, the effect of the moment of inertia has not yet been defined. However, since the moment of inertia can be understand as the difficulty of rotating an object, it is possible to convert it as the torque effect (Section 3.1) such as the friction (Section 3.2). For example, we can convert the inertia as a single large mass

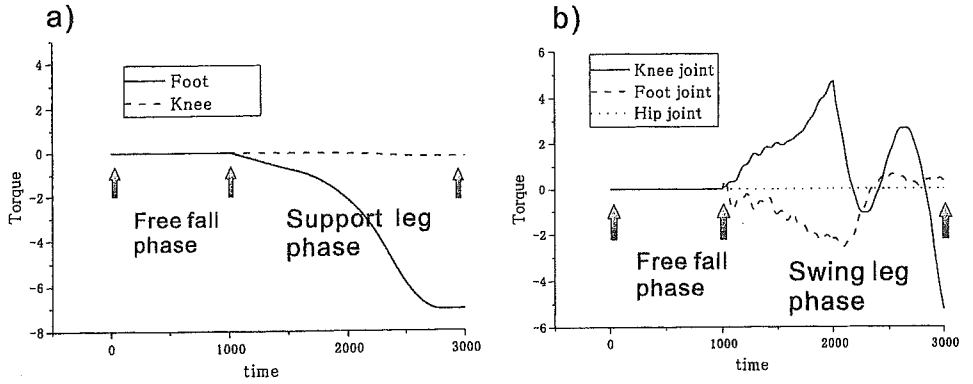

Figure 15. Torque response of the support leg (a) and the swing leg (b) in walking movement (from $t = 0$ to $t = 3000$).

in the case when the center of the rotation is defined. If the mass is positoned at the terminus of the link, we can calculate the conversion mass m:

$$I = m \cdot l^2 \Leftrightarrow m = \frac{I}{l^2} \tag{33}$$

where l is the link length and I is the moment of inertia. By using this method, we can include the effect of the moment of inertia. With regard to the computational cost, the order of the forward kinematics calculations of multi-link system is about $O(n)$ and the order is changed to $O(n^2)$ in the case that there are restriction conditions [9, 10]. However, the order of the our proposed method is $O(n)$ under the restriction conditions and this is another advantage of our proposed method.

7. CONCLUSIONS

In this paper, we propose a new three-dimensional multi-link movement simulator. Our proposed method considers the multi-link system as a multi-particle movement system which each of the particles being connected by a simple spring–damper model. By including the rotation plane in this model, we can treat the revolute joint, and represent the effect of the torque and the friction. By using this assumption, it is not necessary to use the Jacobian matrix for calculating the link dynamics and it is very easy to manage many of external effects, such as the floor, external shock or gravity effect, as external forces toward each of the particles. These features play an important role in the complex dynamics simulation of the multi-link system, especially in the case of a large numner of links. Through experiments with the multi-link dynamics simulation, we confirmed the effectiveness of the proposed method. This means that the work space representation of the multi-link system is more useful for the movement dynamics simulation as compared with the angle state space representation.

REFERENCES

1. Y. Sugahara, T. Endo, H.-o. Lim and A. Takanishi, Design of a battery-powered multi-purpose bipedal locomotor with parallel mechanism, in *Proc. IEEE/RSJ Int. Conf. on Intelligent Robots and Systems*, pp. 2658–2663 (2002).
2. H. Inoue, HRP: humanoid robotics project of MITI, in *Proc. 1st IEEE–RAS Int. Conf. on Humanoid Robots* (2000).
3. Y. Sakagami, R. Watanabe, C. Aoyama, S. Matsunaga, N. Higaki and K. Fujita, The intelligent ASHIMO: system overview and integration, in *Proc. IEEE/RSJ Int. Conf. on Intelligent Robots and Systems*, pp. 2478–2483 (2002).
4. J.-H. Kim and J.-H. Oh, Torque feedback control of the humanoid platform KHR-1, in *Proc. 3rd IEEE Int. Conf. on Humanoid Robots*, pp. 00–00, Karlsruhe and Munich (2003).
5. T. Inamura, I. Toshima and Y. Nakamura, Acquisition and embodiment of motion elements in closed mimesis loop, in *Proc. IEEE Int. Conf. on Robotics and Automation*, pp. 1539–1544 (2002).
6. F. Kanehiro, K. Fujiwara, S. Kajita, K. Yokoi, K. Kaneko and H. Hirukawa, Open architecture humanoid robot platform, in *Proc. Int. Conf. on Robotics and Automation* (2002).
7. S. Kajita, O. Matsumoto and M. Saigo, Real-time 3D walking pattern generation for a biped robot with telescopic legs, in *Proc. IEEE Int. Conf. on Robotics and Automation*, pp. 2299–2036 (2001).
8. K. Yamane and Y. Nakamura, Dynamic filter — concept and implementation of on-line motion generator for human figures, in *Proc. IEEE Int. Conf. on Robotics and Automation*, pp. 688–695, San Francisco, CA (2000).
9. R. Featherstone, *Robot Dynamics Algorithms*, Kluwer, Dordrecht (1987).
10. M. W. Walker and D. E. Orin, Efficient dynamic computer simulation of robotic mechanisms, *J. Dyn. Syst. Meas. Control* **104**, 205–211 (1982).
11. K. Yamane and Y. Nakamura, Dynamics filter oncept and implementation of on-line motion generator for human figures, in *Proc. IEEE Int. Conf. on Robotics and Automation*, pp. 688–694 (2000).
12. Y. Fujimoto and A. Kawamura, Simulation of an autonomous biped walking robot including environmental force interaction, *IEEE Robotics Automat. Mag.* (June), 33–42 (1998).
13. M. Vukobratovic and J. Stepanenko, On the stability of anthropomorphic systems, *Math. Biosci.* **15**, 1–37 (1972).

ABOUT THE AUTHORS

Hideki Toda belongs to the Doctoral Program of Systems and Information Engineering of Sankai Laboratory University of Tsukuba, Tsukuba, Japan.

Yoshiyuki Sankai received the PhD degree in Engineering from the University of Tsukuba, Japan in 1987. He was named a JSPS fellow, Research Associate and Associate Professor in University of Tsukuba. He is a Visiting Professor at Baylor College of Medicine, USA and Ordinary Professor at the Institute of Systems and Engineering Mechanics, University of Tsukuba, Japan. His research interests include assistive exoskeletal robots, the next generations of artificial hearts and humanoids as related fields of cybernetics. He received the JSAO Grant of the Japanese Society for Artificial Organs, and Awards from the American Society for Artificial Organs, International Society for Artificial Organs and International Society for Rotary Blood Pump with his students. He is a Chair of Japan Society of Embolus Detection and Treatment, Vice Chair of the International Journal of the Robotics Society of Japan, Member of the Awards Committee of the Japan Society of Mechanical Engineers, and Member of the Assessment Committee of the New Energy and Industrial Technology Development Organization, Japan.